



Published in final edited form as:

Mol Cell. 2008 December 26; 32(6): 791–802. doi:10.1016/j.molcel.2008.10.028.

Structural and Functional Analysis of the *E. coli* NusB-S10 Transcription Antitermination Complex

Xiao Luo¹, He-Hsuan Hsiao², Mikhail Bubunenکو^{3,4}, Gert Weber¹, Donald L. Court³, Max E. Gottesman^{5,*}, Henning Urlaub², and Markus C. Wahl^{1,6,*}

¹ Max-Planck-Institute for Biophysical Chemistry, Research Group X-Ray Crystallography

² Research Group Bioanalytical Mass Spectrometry, Am Faßberg 11, D-37077 Göttingen, Germany

³ Gene Regulation and Chromosomal Biology Laboratory, Center for Cancer Research, National Cancer Institute at Frederick, Maryland 21702, USA

⁴ Basic Research Program, SAIC-Frederick, Inc., NCI-Frederick, Frederick, Maryland 21702, USA

⁵ Columbia University Medical Center, Departments of Microbiology and Biochemistry and Molecular Biophysics, New York, New York 10032, USA

⁶ Georg-August-University Göttingen, Department of Medicine, Justus-von-Liebig-Weg 11, D-37077 Göttingen, Germany

Summary

Protein S10 is a component of the 30S ribosomal subunit and participates together with NusB protein in processive transcription antitermination. The molecular mechanisms by which S10 can act as a translation or a transcription factor are not understood. We used complementation assays and recombineering to delineate regions of S10 dispensable for antitermination, and determined the crystal structure of a transcriptionally active NusB-S10 complex. In this complex, S10 adopts the same fold as in the 30S subunit and is blocked from simultaneous association with the ribosome. Mass spectrometric mapping of UV-induced crosslinks revealed that the NusB-S10 complex presents an intermolecular, composite and contiguous binding surface for RNAs containing BoxA antitermination signals. Furthermore, S10 overproduction complemented a *nusB* null phenotype. These data demonstrate that S10 and NusB together form a BoxA-binding module; that NusB facilitates entry of S10 into the transcription machinery; and that S10 represents a central hub in processive antitermination.

Introduction

As one strategy to increase the functional diversity of their proteomes, organisms make use of “moonlighting” proteins that can function in more than one cellular context (Jeffery, 1999). In many cases, the molecular basis for the dual activity of a particular protein is unknown. Prime among such multi-purpose proteins are the ribosomal (r-) proteins, many of which exhibit additional extra-ribosomal functions (Wool, 1996). For example, transcription and translation are directly coupled in prokaryotes and a number of r-proteins moonlight as transcription

*To whom correspondence should be addressed. MEG: Tel.: ++1-212-305-6900, Fax: ++1-212-1741; eMail: meg8@columbia.edu, MCW: Tel.: ++49-551-201-1046; Fax: ++49-551-201-1197; eMail: mwahl@gwdg.de.

Publisher's Disclaimer: This is a PDF file of an unedited manuscript that has been accepted for publication. As a service to our customers we are providing this early version of the manuscript. The manuscript will undergo copyediting, typesetting, and review of the resulting proof before it is published in its final citable form. Please note that during the production process errors may be discovered which could affect the content, and all legal disclaimers that apply to the journal pertain.

factors (Squires and Zaporozets, 2000). As the first such example, bacterial S10 was initially defined as an r-protein before an additional role in transcription was discovered (Friedman et al., 1981).

During lytic growth, phage λ switches from early to delayed early gene expression by processive transcription antitermination, which relies on the phage-encoded protein N, an RNA control sequence (N-utilization site, Nut; comprising two linear elements, BoxA and a “spacer”, followed by a stem-loop, BoxB) and four host N-utilization substances (NusA, B, E and G) (Friedman and Court, 1995; Friedman and Gottesman, 1983). NusE is identical to r-protein S10 (Friedman et al., 1981). N, Nut RNA and the Nus factors form a ribonucleoprotein complex on the surface of RNA polymerase (RNAP), in which RNA and protein factors engage in numerous, predominantly weak and cooperative contacts (Mogridge et al., 1995). The N-Nut-Nus factor complex accompanies RNAP during elongation *via* RNA looping (Whalen and Das, 1990) and promotes progressive transcription elongation through downstream intrinsic and factor-dependent termination sites (Weisberg and Gottesman, 1999). *Escherichia coli* and other bacteria utilize a similar mode of processive antitermination during rRNA gene (*rrn*) transcription (Li et al., 1984; Quan et al., 2005). Other r-proteins, including S4, additionally participate in this latter process (Torres et al., 2001). In contrast, prophage HK022, to avoid superinfection by λ , expresses the Nun protein, a transcription factor related to N, which competes with N at λ Nut sites and, after enlisting the four Nus factors, provokes transcription termination on the λ chromosome (Robert et al., 1987).

S10 is an important architectural element in the 30S ribosomal subunit, as revealed by reconstitution (Mizushima and Nomura, 1970) and crystal structure analyses (Schlunzen et al., 2000; Wimberly et al., 2000). During antitermination, S10 forms a stable complex with NusB (Mason et al., 1992) that has enhanced affinity for BoxA-containing RNAs compared to NusB alone (Lüttgen et al., 2002; Mogridge et al., 1998; Nodwell and Greenblatt, 1993). Since BoxA is strictly conserved in all seven *rrn* operons of *E. coli* whereas the BoxB-like element is dispensable for *rrn* antitermination (Berg et al., 1989), association of NusB, S10 and BoxA is considered as a key nucleation event during processive antitermination (Greive et al., 2005).

Presently, it is unclear how S10 is reprogrammed as a transcription factor. In particular, it is unknown how S10 interacts with NusB, whether the conformation of S10 in transcription is different from that in the 30S subunit (Gopal et al., 2001), whether the protein can remain part of the ribosome while participating in antitermination (Das et al., 1985) and why a NusB-S10 complex exhibits enhanced affinity for BoxA RNA. Here, we present genetic, biochemical and structural data that address these questions. Our results redefine the roles of S10 and NusB during transcription regulatory processes.

Results

The Long Ribosome-Binding Loop of S10 Is Dispensable for Transcriptional Functions

To investigate the structural requirements of S10 as a transcription factor, we attempted to delineate molecular regions that are dispensable for processive transcription antitermination. In the 30S subunit, S10 exhibits a globular domain that is located at the surface of the particle and an extended ribosome-binding loop that penetrates the subunit and interacts with several other r-proteins and the 16S rRNA (Schlunzen et al., 2000; Wimberly et al., 2000). We speculated that the ribosome-binding loop may be dispensable for transcription antitermination. To test this idea, we generated a truncated S10 variant, in which this loop (residues 46–67) was replaced by a serine (S10 ^{Δ loop}). To test whether the truncation affected the interaction with NusB, full-length S10 or S10 ^{Δ loop} were co-expressed with NusB in *E. coli* and purified *via* a GST-tag on the S10 molecules. Both wild type (wt) and truncated S10

remained stably associated with NusB during purification (Figure 1A, lanes 1–6). During antitermination, the NusB-S10 complex interacts with the BoxA RNA element, a function that should be preserved in the NusB-S10^{Δloop} complex. Indeed, the affinities of the full-length and loop-deleted complexes for BoxA-containing RNAs were comparable in a filter-binding assay (Figure 1B). We also tested the antitermination activity of the loop-deleted S10 variant directly. S10^{Δloop} complemented λ growth at 42 °C in an *E. coli* strain bearing a chromosomal *nusE71* defect (Table 1) that normally blocks N-antitermination and λ growth at high temperatures (Friedman et al., 1981) (herein, we refer to the genes encoding S10 or S10^{Δloop} and their variants as *nusE* or *nusE*^{Δloop}, rather than *rpsJ* or *rpsJ*^{Δloop}, respectively). Therefore, the antitermination activity of S10 is unaffected by deletion of its ribosome-binding loop.

Next, we used recombineering to ask whether *nusE*^{Δloop} is able to suppress deletion of the chromosomal *nusE* gene, which is essential for cell growth (Bubunencko et al., 2007). In cells containing a plasmid with *nusE* under arabinose control, the chromosomal *nusE* could be replaced with a *kan* gene, conferring kanamycin resistance, in an arabinose-dependent manner (Figure 1C). In contrast, cells containing plasmid-borne *nusE*^{Δloop} yielded only rare *nusE* \leftrightarrow *kan* recombinants irrespective of arabinose induction. The forty such recombinants tested all carried an additional *nusE*⁺ gene as a tandem duplicate in the chromosome. Thus, *nusE*^{Δloop} does not encode all vital functions of *nusE*. Most likely the flexible loop is essential for cell growth due to its role in the ribosome. These data show that transcriptional and translational functions can be partially attributed to distinct regions of S10.

Crystal Structure of a Transcriptionally Active NusB-S10 Complex

We exploited the results from the functional dissection of S10 in order to devise a high-resolution crystal structure of a transcriptionally active NusB-S10 complex. Crystals obtained from the complex of the full-length proteins did not diffract well. We reasoned that the ribosome-binding loop of S10 might be flexible off the ribosome and disturb the crystalline order. Indeed, the NusB-S10^{Δloop} complex gave rise to crystals that diffracted to 1.3 Å resolution and allowed structure solution by molecular replacement. The structure was refined to R_{work} and R_{free} factors of 17.3 and 20.4 %, respectively (Supplemental Data, Table 2).

In the structure of the complex (Figure 2A), NusB adopts an all-helical fold with two perpendicular three-helix bundles. S10^{Δloop} exhibits a four-stranded antiparallel β -sheet backed by two α -helices on one side. Helix α 1 and an irregular strand, β 2, of S10^{Δloop} bridge the two helical bundles of NusB (contact regions I and II in Figure 2A). The region on NusB contacted by S10^{Δloop} coincides with NusB residues that show NMR chemical shift changes upon addition of full-length S10 (Das et al., 2008). These observations further corroborate the equivalence of the wt and loop-deleted S10 in transcription.

NusB and S10^{Δloop} approach each other *via* complementary electrostatic surfaces (Figure 2B), burying ca. 1700 Å² of combined surface area upon complex formation. The two proteins engage in mixed hydrophobic and hydrophilic interactions (Figure 2C-F). For example, an intramolecular Asp19-Arg72 ion pair of S10^{Δloop} forms hydrogen bonds to Tyr18 of NusB, thereby positioning Tyr18 between Pro39 and Pro41 of a proline motif (Pro39-Ile40-Pro41-Leu42-Pro43) on strand β 2 of S10 (Figure 2C). The remainder of the proline motif with two intervening apolar side chains engages in snug van-der-Waals contacts with NusB-Phe114, sandwiching it between S10-Pro41 and S10-Pro43 (Figure 2D). Pro39 is molded into a *cis* conformation that allows it to participate in intra- and intermolecular hydrogen bonding networks (Figure 2E).

NusB and S10 Retain their Overall Folds upon Complex Formation but Interact *via* Local Induced Fit

The global structures of isolated NusB (Altieri et al., 2000; Bonin et al., 2004; Das et al., 2008; Gopal et al., 2000) and of NusB in complex with S10^{Δloop} are very similar (Figure 2A, inset 1; Table S1). S10^{Δloop} in complex with NusB likewise resembles the structure of S10 in the 30S subunit (Schuwirth et al., 2005) (Figure 2A, inset 2; Table S1). The fold of S10 by itself is unstable (Das et al., 2008; Gopal et al., 2001); thus, NusB apparently acts to stabilize S10 in the same overall conformation it takes in the ribosome. Clearly, our data exclude the possibility that S10 is extensively remodeled by NusB as a mechanism for partitioning of S10 between the translation and transcription machineries.

While the global structures of both proteins are conserved, they are apparently adjusted by local induced fit upon complex formation. A pronounced difference to the structure of NusB determined in isolation (Altieri et al., 2000; Bonin et al., 2004; Das et al., 2008; Gopal et al., 2000) is seen in the loop connecting helices $\alpha 4$ and $\alpha 5$, which rearranges to allow an ionic interaction between NusB-Glu75 and S10-Arg16 (Figure 3A). In agreement with this observation, strong NMR chemical shift changes were previously observed in this loop of NusB upon addition of full-length S10 (Das et al., 2008). In ribosome-bound S10 (Schuwirth et al., 2005; Selmer et al., 2006; Wimberly et al., 2000) several residues that contact the 16S rRNA, including Pro39 and Arg72, have been refined with different conformations compared to the present structure of S10 in complex with NusB. While these data suggest that S10 also adjusts locally to accommodate different binding partners, the limited resolution of the ribosome structures precludes a more detailed comparison.

Binding of S10 to NusB is Mutually Exclusive with its Incorporation into the Ribosome and With NusB Dimerization

S10 residues His15, Arg37, Pro39, Ile40, Pro41, Pro43, Thr44, His70 and Arg72, which directly interact with NusB, also directly contact 16S rRNA in the 30S subunit (within 3.5 Å distance; (Schuwirth et al., 2005)). As a consequence, the surface of S10 that binds NusB is occluded in the ribosome (Figure 3B). Thus, contrary to a previous hypothesis (Das et al., 1985; Gopal et al., 2001), S10 cannot participate with NusB in transcription antitermination as a part of the 30S subunit. This finding is in agreement with the observation that processive N-dependent antitermination can be reconstituted using purified S10 and other Nus factors (Das et al., 1985).

Mycobacterium tuberculosis NusB forms dimers (Gopal et al., 2000) whose significance for transcription antitermination has so far remained obscure. Comparison of these dimers to our NusB-S10^{Δloop} complex shows that NusB dimerization would interfere with S10 binding (Figure 3C). This observation is in agreement with our previous suggestion (Bonin et al., 2004) that dimerization may be used as a packaging mechanism by some organisms to downregulate aberrant activities of isolated NusB. Similar autoinhibitory mechanisms have been demonstrated for other transcription antitermination factors (Belogurov et al., 2007; Mah et al., 2000).

Molecular Basis of the *nusB5* and *nusE100* Phenotypes

Mutations in *nusB* and *nusE* have served as important genetic tools to study processive antitermination. However, the biochemical basis for the dysfunction or suppressor activity of any of the mutant proteins was not defined. The *nusB5* allele gives rise to a Tyr18Asp mutation in NusB (Court et al., 1995) and leads to a defect in N-dependent antitermination that blocks λ growth (Friedman et al., 1976). The *nusE100* mutation restricts Nun-termination but not N-antitermination (Robledo et al., 1991). We have sequenced the *nusE100* allele and find that it encodes an S10^{Arg72Gly} variant. Remarkably, NusB-Tyr18 and S10-Arg72 are both involved

in the same buried, hydrophilic, intermolecular interaction network at the center of the NusB-S10 interface (Figure 2C). Replacement of NusB-Tyr18 by Asp or replacement of S10-Arg72 by Gly is expected to interfere with this interaction network. Therefore, it is possible that the defects of the mutant alleles are in part caused by a weakened NusB-S10 affinity. We tested this idea by monitoring the ability of the mutant proteins to sustain NusB-S10 interaction in GST-pull down assays. Indeed, the NusB5 variant (Tyr18Asp) did not bind to S10^{Δloop} (Figure 1A, lanes 7–9) and the S10^{Δloop,Arg72Gly} mutant protein of *nusE100^{Δloop} failed to interact with NusB (lanes 10–12).*

Previously, the lack of production of a stable gene product was thought to be the cause of the *nusB5* defect in N-antitermination (Mason et al., 1992). Our results, in contrast, suggest that *nusB5* gives rise to a gene product that is less active due to a weakened interaction with S10. In that case, the *nusB5* defect may be overcome simply by mass action. Therefore, we asked if high levels of NusB5 can restore N antitermination. Indeed, overexpression of the NusB5 protein in an *E. coli nusB* deletion strain partially rescued λ growth (Table S2). In agreement with this observation, multiple copies of a plasmid carrying the *nusB5* gene have previously been found to complement a chromosomal *nusB5* allele (Court et al., 1995). Thus, our data underscore the importance of a stable NusB-S10 interaction at physiological expression levels of these proteins for N and Nun activities.

The NusB-S10 Complex Exhibits an Intermolecular, Mosaic and Contiguous BoxA RNA-Binding Surface

To explore the mechanism by which S10 enhances the affinity of NusB for BoxA RNA, we investigated how NusB and the NusB-S10 complex interact with BoxA-containing RNA. We exposed NusB-RNA or NusB-S10-RNA complexes to UV light and analyzed by mass spectrometry the zero-length crosslinks generated (Table S3; Figure S1). We employed the same two 19-nucleotide λ NutR BoxA or *rrm* BoxA RNAs, previously used in fluorescence-based interaction studies (Greive et al., 2005) (see Figure 4A). Overall, we identified four peptides in NusB (B1, B1', B2 and B3) and three in full-length S10 (E1, E2 and E3) that crosslinked to distinct, short RNA elements (Figure 4A; Table S3). UV-induced crosslinking in the absence of RNA oligos and mass analysis with complete mixtures but without UV-irradiation did not give rise to any peaks corresponding to those of the identified peptide-RNA crosslinks.

Scrutinizing the sequences of the crosslinked peptides and RNA elements allowed us to deduce unequivocally the molecular neighborhoods (Supplemental Results and Discussion). These data show that NusB is in close proximity to residues 3–8 of *rrm* BoxA and residues 3–9 of λ BoxA, while S10 is in direct contact with residues 8, 9 and 12 of *rrm* BoxA, residues 7, 8 and 12 of λ BoxA and with residues just downstream in either of the RNAs (Figure 4A; Table S3). The BoxA positions in direct contact with NusB and S10 are remarkably congruent with residues 2–9 of *rrm* BoxA and residues 2–7 of λ BoxA, which are essential for recruitment of NusB and S10 to the antitermination machineries (Mogridge et al., 1998). In addition, parts of the S10 ribosome-binding loop (the entire peptide E2 and part of E3) crosslinked to RNA at the very 3'-end of the core BoxA elements and to nucleotides immediately downstream (Figure 4A; Table S3). Thus, the ribosome-binding loop fosters auxiliary, but not essential (Table 1), mRNA contacts that might enhance processive antitermination.

Since we find virtually identical crosslinks of NusB to the RNAs in the absence or in the presence of S10 (Table S3), we conclude that the specificity of the NusB-BoxA RNA contacts is influenced little if at all by S10. Thus, the direct S10-BoxA interactions detected herein are responsible for the increased BoxA RNA affinity of the NusB-S10 complex compared to NusB alone. Since isolated S10 binds RNA weakly and largely non-specifically (Greive et al.,

2005), NusB apparently stabilizes an RNA-binding conformation of S10 and positions S10 on the BoxA RNA, suggesting that NusB loads S10 onto a specific RNA element.

The amino acid residues crosslinked to RNA in both NusB and S10 are dispersed in the primary sequences but nevertheless coalesce in 3D on one surface of the NusB-S10^{Δloop} complex (Figure 4A). Peptides B1 (B1'), B2 and B3 form a contiguous surface on NusB and peptide E1 of S10 directly neighbors the C-terminus of peptide E3 at the base of the ribosome-binding loop. The tip of NusB peptide B2 is in weak direct contacts with S10 peptides E1 and E3 (Figure 4A). Thus, NusB and S10 together present a contiguous, mosaic BoxA-binding surface. We combined the results from our structural and crosslinking analyses to derive the overall topology of the NusB-S10-RNA complex (Figure 4A, inset). The central region of a BoxA element is placed on the confluent binding surface of the protein complex. The RNA runs 5'-to-3' from the NusB to the S10 RNA-binding patches.

***nusB101* Represents a Gain-of-Function Mutation with Increased RNA Affinity**

The *nusB101* mutation (Asp118Asn) suppresses the N-antitermination defects of NusA1 and NusE71 mutants at high temperatures (Ward et al., 1983). Notably, NusB-Asp118 is part of peptide B2, which lies at the center of the closely spaced RNA-binding patches on NusB and S10 (Figure 4A). Removal of a negative charge at the NusB-118 position could conceivably increase the RNA affinity of NusB and of the NusB-S10 complex, in agreement with a previous proposal (Court et al., 1995). We tested this idea by crosslinking increasing amounts of NusB-S10^{Δloop} and of NusB101-S10^{Δloop} (NusB^{Asp118Asn}-S10^{Δloop}) to BoxA-containing RNAs under conditions where the crosslink yields reflect the binding equilibria. As predicted, NusB101-S10^{Δloop} exhibited increased affinities for either λ or *rrn* BoxA sequences (Figure 4B; Figure S2). Since both NusB101 and S10 showed increased crosslinking, the difference was not due to direct crosslinking of Asn118 of NusB101 to the RNA. Thus, *nusB101* represents a gain-of-function mutation that increases the affinity of NusB for BoxA. Consistent with cooperativity among the component antitermination factors, enhanced RNA affinity in NusB101 might compensate for decreased RNA affinity of the suppressed NusA1 mutant, in which a core residue of the S1 RNA-binding domain is altered (Worbs et al., 2001).

The *nusE71* Mutation Defines an Additional Interaction Surface on S10

The residue affected by the *nusE71* mutation (Ala86Asp), which blocks both N and Nun, is remote from the NusB interface and the RNA-binding region of S10. We have determined the structure of a NusB-S10^{Δloop,Ala86Asp} complex and find that it is virtually identical to the wt complex (root-mean-square deviation of ca. 0.8 Å for 206 C α atoms; Table 2; Figure 5A). Therefore, dysfunction of S10^{Ala86Asp} is not due to a global effect on the structure of the protein. Rather, the mutation changed the local surface properties of S10 (Figure 5B). This finding suggests that yet another molecular interaction of S10 may be attenuated in S10^{Ala86Asp}. S10 is known to interact directly with RNAP (Mason and Greenblatt, 1991) and it is possible that the helix α 2 region encompassing residue 86 is involved in this association. Alternatively, the S10 region around Ala86 might mark an interface with N and Nun; N and S10 proteins are reported to co-purify in some preparations (Mogridge et al., 1995; Mogridge et al., 1998). This notion would explain the otherwise puzzling observation that *nusE71* does not block *rrn* antitermination, which uses RNAP but not N or Nun (Zellars and Squires, 1999).

S10 Supports Transcription Antitermination in the Absence of NusB

N and *rrn* antitermination and Nun-termination involve appropriate tethering of BoxA and BoxB RNA sites to RNAP *via* N or Nun and the Nus factors (Nodwell and Greenblatt, 1991). Since S10 directly contacts RNA (this work) and RNAP (Mason and Greenblatt, 1991), we considered the possibility that S10 may be the functional antitermination factor in the NusB-S10 complex at Nut sites. To test this idea, we overexpressed S10 and S10^{Δloop} in an *E. coli*

strain lacking the *nusB* gene. Strikingly, overexpression of either S10 or S10^{Δloop} rescued λ growth, restoring functional N-antitermination in the absence of NusB (Table 3). Similarly, S10 or S10^{Δloop} expression rescued Nun-dependent termination in the *nusB*-deletion strain, as determined by the expression of a *lacZ* gene promoter-distal to λ Nut (Table 3). These results are at variance with the traditional view that the role of S10 is to recruit NusB to RNAP (Mason and Greenblatt, 1991; Mason et al., 1992). We propose, therefore, that NusB, although it engages in more extensive BoxA contacts than S10, merely serves as a loading factor that ensures efficient entry of S10 into these transcription complexes, while S10 constitutes the critical antitermination component of the NusB-S10 complex.

Discussion

The balance between transcription termination and progression of transcription (antitermination) is controlled at specific sites in genes. Factor ensembles that interact with RNAP have evolved to interpret such control sites. One example is the antitermination machinery that regulates the transcription of the phage λ genome and of rRNA genes in bacteria. The molecular mechanisms underlying this fundamental regulatory principle of transcription are incompletely understood. Here, we have presented work that redefines the roles of a r-protein, S10, which is part of these antitermination complexes, and of another antitermination factor, NusB, which forms a stable sub-complex with S10. Apart from the implications for a fundamental transcription regulatory principle, our results have repercussion for the generation of functional diversity in proteomes by employing one protein, S10, for multiple activities.

S10^{Δloop} is a Tool to Dissect Translational and Transcriptional Functions of S10

We have delineated structural elements of S10 that are exclusively required for S10 function in the ribosome but not in transcription. Our finding that the long loop of S10 is dispensable in transcription is consistent with the observation that mutants defective in transcriptional functions (*nusE71*, *nusE100*) map to the globular part of S10. The functional architecture of S10 is paralleled by that of r-protein L4, which also has a second activity as a transcriptional attenuator (Lindahl et al., 1983). In L4, a similar ribosome-binding loop was also found dispensable for attenuation (Worbs et al., 2000; Zengel et al., 2003). Our findings show that evolution made economic use of r-proteins by diverting regions not under strict selection by ribosomal functions to other purposes.

The S10 loop is of obvious architectural importance for the 30S subunit (Schluenzen et al., 2000; Wimberly et al., 2000), consistent with our observation that the loop is essential for cell viability. These results suggest that the transcription antitermination activity of S10 is independent of ribosomes or ribosome-bound S10, in agreement with our finding that S10 cannot bind to NusB and the 30S subunit at the same time. The above results also suggest that under normal growth conditions, rRNA transcription antitermination is not essential and that proteins involved in antitermination are required because of their role in other cellular processes, as recently also shown for other antitermination factors (Bubunencko et al., 2007; Phadtare et al., 2007).

S10 Is Adapted to Different Functional Contexts without Global Structural Remodeling

Since its fold is unstable, S10 has been suggested to represent a largely intrinsically unstructured protein, whose structure could adapt to different functional contexts (Gopal et al., 2001). S10 expressed alone exhibits low solubility and tends to aggregate. NusB confers increased solubility on S10 (Figure 1A), suggesting that S10 may preferentially exist in complex with NusB off the ribosome. We observe that the bulk of S10 adopts the same global fold in complex with NusB as in the ribosome. Thus, our results rigorously exclude the possibility that the structure of S10 is extensively remodeled in order to recruit the protein as

a transcription factor. Indeed, the long ribosome-binding loop is most likely the only intrinsically unfolded region of S10.

Mutually Exclusive Binding of S10 to the 30S Subunit or NusB May Provide for Feedback Control of Ribosome Biogenesis

Balancing the levels of ribosomal building blocks is critical for bacteria, since ribosome biosynthesis can consume half of the available metabolic energy (Bremer and Dennis, 1987). A number of negative feedback loops have been characterized that act to ensure stoichiometric levels of ribosomal constituents. When expressed in surplus of their rRNA binding sites, several r-proteins restrict their own expression and that of other proteins in their operons by binding to their own mRNAs, thereby sequestering the messages from translation (Lindahl and Zengel, 1986). In addition to such translational feedback, r-protein L4 also down-regulates transcription of its operon (Lindahl et al., 1983). Evidence presented here suggests that such negative feedback may be complemented by positive feedback through r-protein S10. Since crystal structures show that S10 cannot participate in transcription antitermination on RNA polymerase and translation on the ribosome at the same time, only S10 produced in excess of ribosomes will elicit antitermination of *rrn* operons and thus a higher rate of rRNA biosynthesis. As a consequence, surplus S10 would act to increase rRNA levels. With respect to rRNA production, NusB and BoxA may therefore be envisioned as enhancers of an S10-based feedback regulation.

S10 and NusB Form a Functional Module for Recognition of BoxA

Much of the proteome is organized as functional modules (Hartwell et al., 1999), which support an autonomous function as, for example, devices within a macromolecular machine. Here we show how the NusB-S10 complex acts as a functional RNA-binding module of the transcriptional machineries with which it is associated. We find that both subunits of the NusB-S10 complex contribute to a mosaic yet contiguous binding surface for a crucial RNA signaling element, BoxA. An analogous situation was encountered intramolecularly in NusA, in which different RNA-binding domains come together to create an enlarged, composite RNA-binding site (Beuth et al., 2005; Worbs et al., 2001). Cooperation between two or more subunits to generate a composite binding surface for an additional factor is an important architectural principle in macromolecular assemblies (Liu et al., 2007).

A Shift in Paradigm: S10 Is the Active Antitermination Factor of the NusB-S10 Complex

In the traditional view of processive antitermination, S10 serves as an auxiliary factor that recruits the antitermination factor NusB to RNAP (Mason and Greenblatt, 1991; Mason et al., 1992). Contrary to that view, we show that S10 supports N-antitermination and Nun-termination even in the absence of NusB. According to our work, NusB has supportive functions, while the fundamental antitermination activity of the complex relies on S10. What are the supportive functions of NusB and what constitutes the fundamental antitermination activity of S10?

S10 is a truly multi-functional protein even within transcriptional complexes. Apart from interacting with NusB (Mason et al., 1992) and this work), it directly binds RNAP (Mason and Greenblatt, 1991). Furthermore, S10 has been suggested to contact phage λ protein N (Mogridge et al., 1995; Mogridge et al., 1998). Our work shows that S10 is even more versatile and also binds to the BoxA RNA element. Thus, S10 constitutes a hub within the N- and *rrn* antitermination and Nun-termination complexes, through which the functions of other factors may be integrated. However, isolated S10 binds RNA with low specificity (Greive et al., 2005). Under physiological conditions, positioning of S10 on the mRNA by RNAP or the phage proteins is presumably inefficient. NusB is therefore required as an adaptor that ensures

efficient loading of S10 on the nascent RNA at BoxA and subsequent contact with RNA polymerase.

Experimental Procedures

Details of molecular biology, protein production, GST pull-down, filter-binding and crystallographic procedures are given in the Supplemental Experimental Procedures.

Gene Essentiality Assay

The functionality of the S10^{Δloop} mutant for cell growth was analyzed using a gene essentiality assay based on recombineering (Bubunenko et al., 2007), as recently described for IF1 mutants (Phadtare et al., 2007). Briefly, recombinogenic DY330 cells containing the *λ red* genes were transformed with pBAD plasmids expressing either S10^{Δloop} or wt S10 as a positive control. Cells were then subjected to recombineering to replace the chromosomal *nusE* open reading frame by fusing its first 15 codons to the *kan* open reading frame (*nusE*_{15-kan}). The *kan* PCR fragment amplified for recombineering was flanked with *nusE* homologous regions using primers 5'

ATGCAGAACCAAAGAATCCGTATCCGCCTGAAAGCGTTTGATCATATTGAA
CAAGATGGATTGCACGC and 5'

CAATCATTGTTTCAACCTCTCAATCGCTCAATGACCTGATCAGAAGAAGTTCG
TCAAGAAG (*nusE* regions in bold). Recombinants were selected on L plates with 25 μg/ml kanamycin and with or without 0.2 % arabinose. Kanamycin-resistant recombinants were analyzed by PCR for the configuration of the targeted *nusE* chromosomal region using a pair of primers flanking the *nusE* gene: 5'TAGCCGAATTTGGCTACCTAACAAAT and 5'GAAGGTAGTTTCGGAAACAGTCAG. The appearance of a single *nusE*<>*kan* fragment indicates that S10 expressed from a plasmid is functional and is able to complement the nonviable chromosomal *nusE* knockout (Bubunenko et al., 2007). The appearance of two fragments representing *nusE*<>*kan* and *nusE* indicates that the S10^{Δloop} copy expressed from a plasmid is not functional and is unable to complement a chromosomal *nusE* knockout. Thus, in this case, recombinants are rare and have a knocked out copy and a wt copy of *nusE*, which reflects the special diploid nature of these strains (Bubunenko et al., 2007).

UV-Induced Crosslinking Assay

Varying concentrations (0, 0.15, 0.31, 0.62, 1.25 and 2.5 μM) of NusB-S10^{Δloop} or NusB101-S10^{Δloop} (NusB^{Asp118Asn}-S10^{Δloop}) were mixed with [³²P]-labeled RNA oligonucleotide in 10 μl reaction volumes and exposed to 254 nm UV light for 5 min at 4 °C (Lingel et al., 2003). Reactions were analyzed by 15 % SDS PAGE. Gels were dried and developed on a phosphoimager. Under saturating conditions, a maximum of ca. 7 % of the total radioactivity was shifted on gels. For quantification, 0.31 and 0.62 μM of NusB-S10^{Δloop} or NusB101-S10^{Δloop} were crosslinked as above. Crosslinked samples from three independent experiments were analyzed on the same SDS gel. For loading control, each sample was divided and averaged. Radiolabeled bands were quantified by densitometry using Image Quant software (GE Healthcare). Crosslink yields for the components of the wt NusB-based complex were normalized to 1 and the yields for the corresponding components of the NusB^{Asp118Asn}-based complex were represented relative to the wt sample.

Mass Spectrometric Analysis of UV-Induced Crosslinking Sites

Eight nmoles of RNA oligomer were incubated with four nmoles of recombinant NusB or NusB-S10 complex in 300 μl of crystallization buffer and exposed to 254 nm UV light for 5 min at 4 °C. Crosslinked samples were precipitated with three volumes of ethanol, dried in a speed vac and dissolved in 50 mM Tris-HCl, pH 7.9, 4 M urea. The urea concentration was adjusted to 1 M and the RNA oligonucleotides were hydrolyzed with 1 μg each of RNases A

and T1 for 2 hours at 52 °C. Trypsin was added to a final ratio of 1:20 (enzyme:substrate) prior to overnight incubation at 37 °C.

The samples were desalted and enriched for crosslinks using TiO₂ micro-columns generated inhouse and injected onto a nano-liquid chromatography (nanoLC) system (Agilent) equipped with a C18 trapping column (Maisch) in line with an analytical C18 column (200 mm × 0.075 mm) packed inhouse. nanoLC separation and electrospray ionization-tandem mass spectrometry were performed with a Q-ToF Ultima mass spectrometer (Waters) as described elsewhere (Deckert et al., 2006).

Supplementary Material

Refer to Web version on PubMed Central for supplementary material.

Acknowledgements

We thank Elke Penka and Monika Raabe (Max-Planck-Institute for Biophysical Chemistry, Göttingen, Germany) for excellent technical assistance, the staff at beamlines PXI/II (SLS, Villigen, Switzerland) and BL14.2 (BESSY, Berlin, Germany) for support during diffraction data collection and Andrew Byrd and Amanda Altieri (NCI, Frederick, MD, USA) for communication of results prior to publication. MCW was supported by grant WA 1126/3-1 from the Deutsche Forschungsgemeinschaft. MEG was supported by NIH grant GM37219. HU was supported by a young investigator grant of EURASNET. This research was supported in part by the Intramural Research Program of the NIH, National Cancer Institute, Center for Cancer Research and by a Trans NIH/FDA Intramural Biodefense Program Grant from NIAID to DLC. This project was funded in part with federal funds from the National Cancer Institute, National Institutes of Health, under contract N01-CO-12400. The content of this publication does not necessarily reflect the views or policies of the Department of Health and Human Services, nor does mention of trade names, commercial products, or organizations imply endorsement by the U.S. Government. Coordinates and structure factors have been deposited with the RCSB Protein Data Bank (<http://www.rcsb.org/pdb/>) under accession codes 3D3B (NusB-S10 Δ loop) and 3D3C (NusB-S10 Δ loop,Ala86A Δ sp) and will be released upon publication. The authors declare that they have no competing financial interests.

References

- Altieri AS, Mazzulla MJ, Horita DA, Heath Coats R, Wingfield PT, Das A, Court DL, Byrd AR. The structure of the transcriptional antiterminator NusB from *Escherichia coli*. *Nat Struct Biol* 2000;7:470–474. [PubMed: 10881193]
- Belogurov GA, Vassilyeva MN, Svetlov V, Klyuyev S, Grishin NV, Vassilyev DG, Artsimovitch I. Structural basis for converting a general transcription factor into an operon-specific virulence regulator. *Mol Cell* 2007;26:117–129. [PubMed: 17434131]
- Berg KL, Squires C, Squires CL. Ribosomal RNA operon anti-termination. Function of leader and spacer region box B-box A sequences and their conservation in diverse micro-organisms. *J Mol Biol* 1989;209:345–358. [PubMed: 2479752]
- Beuth B, Pennell S, Arnvig KB, Martin SR, Taylor IA. Structure of a *Mycobacterium tuberculosis* NusA-RNA complex. *EMBO J* 2005;24:3576–3587. [PubMed: 16193062]
- Bonin I, Robelek R, Benecke H, Urlaub H, Bacher A, Richter G, Wahl MC. Crystal structures of the antitermination factor NusB from *Thermotoga maritima* and implications for RNA binding. *Biochem J* 2004;383:419–428. [PubMed: 15279620]
- Bremer, H.; Dennis, PP. Modulation of chemical composition and other parameters of the cell by growth rate. In: Neidhardt, FC.; Ingraham, JL.; Low, KB.; Magasanik, B.; Schaechter, M.; Umberger, HE., editors. *Escherichia coli* and *Salmonella thyphimurium*: Cellular and molecular biology. Washington, DC, USA: American Society for Microbiology; 1987. p. 1527-1542.
- Bubunenko M, Baker T, Court DL. Essentiality of ribosomal and transcription antitermination proteins analyzed by systematic gene replacement in *Escherichia coli*. *J Bacteriol* 2007;189:2844–2853. [PubMed: 17277072]
- Court DL, Patterson TA, Baker T, Costantino N, Mao X, Friedman DI. Structural and functional analyses of the transcription-translation proteins NusB and NusE. *J Bacteriol* 1995;177:2589–2591. [PubMed: 7730297]

- Das A, Ghosh B, Barik S, Wolska K. Evidence that ribosomal protein S10 itself is a cellular component necessary for transcription antitermination by phage lambda N protein. *Proc Natl Acad Sci USA* 1985;82:4070–4074. [PubMed: 2987961]
- Das R, Loss S, Li J, Waugh DS, Tarasov S, Wingfield PT, Byrd RA, Altieri AS. Structural biophysics of the NusB:NusE antitermination complex. *J Mol Biol* 2008;376:705–720. [PubMed: 18177898]
- Deckert J, Hartmuth K, Boehringer D, Behzadnia N, Will CL, Kastner B, Stark H, Urlaub H, Lührmann R. Protein composition and electron microscopy structure of affinity-purified human spliceosomal B complexes isolated under physiological conditions. *Mol Cell Biol* 2006;26:5528–5543. [PubMed: 16809785]
- Friedman DI, Baumann M, Baron LS. Cooperative effects of bacterial mutations affecting lambda N gene expression. I Isolation and characterization of a nusB mutant. *Virology* 1976;73:119–127. [PubMed: 785802]
- Friedman DI, Court DL. Transcription antitermination: the lambda paradigm updated. *Mol Microbiol* 1995;18:191–200. [PubMed: 8709839]
- Friedman, DI.; Gottesman, ME. Lytic mode of lambda development. In: Hendrix, RW.; Roberts, JW.; Stahl, FW.; Weisberg, RA., editors. *Lambda II*. Cold Spring Harbor, N.Y.: Cold Spring Harbor Laboratory Press; 1983. p. 21–51.
- Friedman DI, Schauer AT, Baumann MR, Baron LS, Adhya SL. Evidence that ribosomal protein S10 participates in control of transcription termination. *Proc Natl Acad Sci USA* 1981;78:1115–1118. [PubMed: 6453343]
- Gopal B, Haire LF, Cox RA, Jo Colston M, Major S, Brannigan JA, Smerdon SJ, Dodson G. The crystal structure of NusB from *Mycobacterium tuberculosis*. *Nat Struct Biol* 2000;7:475–478. [PubMed: 10881194]
- Gopal B, Papavinasundaram KG, Dodson G, Colston MJ, Major SA, Lane AN. Spectroscopic and thermodynamic characterization of the transcription antitermination factor NusE and its interaction with NusB from *Mycobacterium tuberculosis*. *Biochemistry* 2001;40:920–928. [PubMed: 11170413]
- Greive SJ, Lins AF, von Hippel PH. Assembly of an RNA-protein complex. Binding of NusB and NusE (S10) proteins to boxA RNA nucleates the formation of the antitermination complex involved in controlling rRNA transcription in *Escherichia coli*. *J Biol Chem* 2005;280:36397–36408. [PubMed: 16109710]
- Hartwell LH, Hopfield JJ, Leibler S, Murray AW. From molecular to modular cell biology. *Nature* 1999;402:C47–52. [PubMed: 10591225]
- Jeffery CJ. Moonlighting proteins. *Trends Biochem Sci* 1999;24:8–11. [PubMed: 10087914]
- Li SC, Squires CL, Squires C. Antitermination of *E. coli* rRNA transcription is caused by a control region segment containing lambda nut-like sequences. *Cell* 1984;38:851–860. [PubMed: 6091902]
- Lindahl L, Archer R, Zengel JM. Transcription of the S10 ribosomal protein operon is regulated by an attenuator in the leader. *Cell* 1983;33:241–248. [PubMed: 6380754]
- Lindahl L, Zengel JM. Ribosomal genes in *Escherichia coli*. *Annu Rev Genet* 1986;20:297–326. [PubMed: 2434021]
- Lingel A, Simon B, Izaurralde E, Sattler M. Structure and nucleic-acid binding of the *Drosophila* Argonaute 2 PAZ domain. *Nature* 2003;426:465–469. [PubMed: 14615801]
- Liu S, Li P, Dybkov O, Nottrott S, Hartmuth K, Lührmann R, Carlomagno T, Wahl MC. Binding of the human Prp31 Nop domain to a composite RNA-protein platform in U4 snRNP. *Science* 2007;316:115–120. [PubMed: 17412961]
- Lüttgen H, Robelek R, Muhlberger R, Diercks T, Schuster SC, Kohler P, Kessler H, Bacher A, Richter G. Transcriptional regulation by antitermination. Interaction of RNA with NusB protein and NusB/NusE protein complex of *Escherichia coli*. *J Mol Biol* 2002;316:875–885. [PubMed: 11884128]
- Mah TF, Kuznedelov K, Mushegian A, Severinov K, Greenblatt J. The alpha subunit of *E. coli* RNA polymerase activates RNA binding by NusA. *Genes Dev* 2000;14:2664–2675. [PubMed: 11040219]
- Mason SW, Greenblatt J. Assembly of transcription elongation complexes containing the N protein of phage lambda and the *Escherichia coli* elongation factors NusA, NusB, NusG, and S10. *Genes Dev* 1991;5:1504–1512. [PubMed: 1831176]

- Mason SW, Li J, Greenblatt J. Direct interaction between two Escherichia coli transcription antitermination factors, NusB and ribosomal protein S10. *J Mol Biol* 1992;223:55–66. [PubMed: 1731086]
- Mizushima S, Nomura M. Assembly mapping of 30S ribosomal proteins from E. coli. *Nature* 1970;226:1214. [PubMed: 4912319]
- Mogridge J, Mah TF, Greenblatt J. A protein-RNA interaction network facilitates the template-independent cooperative assembly on RNA polymerase of a stable antitermination complex containing the lambda N protein. *Genes Dev* 1995;9:2831–2845. [PubMed: 7590257]
- Mogridge J, Mah TF, Greenblatt J. Involvement of boxA nucleotides in the formation of a stable ribonucleoprotein complex containing the bacteriophage lambda N protein. *J Biol Chem* 1998;273:4143–4148. [PubMed: 9461609]
- Nodwell JR, Greenblatt J. The nut site of bacteriophage lambda is made of RNA and is bound by transcription antitermination factors on the surface of RNA polymerase. *Genes Dev* 1991;5:2141–2151. [PubMed: 1834523]
- Nodwell JR, Greenblatt J. Recognition of boxA antiterminator RNA by the E. coli antitermination factors NusB and ribosomal protein S10. *Cell* 1993;72:261–268. [PubMed: 7678781]
- Phadtare S, Kazakov T, Bubunenko M, Court DL, Pestova T, Severinov K. Transcription antitermination by translation initiation factor IF1. *J Bacteriol* 2007;189:4087–4093. [PubMed: 17384193]
- Quan S, Zhang N, French S, Squires CL. Transcriptional polarity in rRNA operons of Escherichia coli nusA and nusB mutant strains. *J Bacteriol* 2005;187:1632–1638. [PubMed: 15716433]
- Robert J, Sloan SB, Weisberg RA, Gottesman ME, Robledo R, Harbrecht D. The remarkable specificity of a new transcription termination factor suggests that the mechanisms of termination and antitermination are similar. *Cell* 1987;51:483–492. [PubMed: 2822258]
- Robledo R, Atkinson BL, Gottesman ME. Escherichia coli mutations that block transcription termination by phage HK022 Nun protein. *J Mol Biol* 1991;220:613–619. [PubMed: 1831236]
- Schluenzen F, Tocilj A, Zarivach R, Harms J, Gluehmann M, Janell D, Bashan A, Bartels H, Agmon I, Franceschi F, Yonath A. Structure of functionally activated small ribosomal subunit at 3.3 angstroms resolution. *Cell* 2000;102:615–623. [PubMed: 11007480]
- Schuwirth BS, Borovinskaya MA, Hau CW, Zhang W, Vila-Sanjurjo A, Holton JM, Cate JH. Structures of the bacterial ribosome at 3.5 Å resolution. *Science* 2005;310:827–834. [PubMed: 16272117]
- Selmer M, Dunham CM, Murphy FVt, Weixlbaumer A, Petry S, Kelley AC, Weir JR, Ramakrishnan V. Structure of the 70S ribosome complexed with mRNA and tRNA. *Science* 2006;313:1935–1942. [PubMed: 16959973]
- Squires CL, Zaporozhets D. Proteins shared by the transcription and translation machines. *Annual Review of Microbiology* 2000;54:775–798.
- Torres M, Condon C, Balada JM, Squires C, Squires CL. Ribosomal protein S4 is a transcription factor with properties remarkably similar to NusA, a protein involved in both non-ribosomal and ribosomal RNA antitermination. *EMBO J* 2001;20:3811–3820. [PubMed: 11447122]
- Ward DF, DeLong A, Gottesman ME. Escherichia coli nusB mutations that suppress nusA1 exhibit lambda N specificity. *J Mol Biol* 1983;168:73–85. [PubMed: 6224023]
- Weisberg RA, Gottesman ME. Processive antitermination. *J Bacteriol* 1999;181:359–367. [PubMed: 9882646]
- Whalen WA, Das A. Action of an RNA site at a distance: role of the nut genetic signal in transcription antitermination by phage-lambda N gene product. *New Biologist* 1990;2:975–991. [PubMed: 2151659]
- Wimberly BT, Brodersen DE, Clemons WM, Morgan-Warren RJ, Carter AP, Vornrhein C, Hartsch T, Ramakrishnan V. Structure of the 30S ribosomal subunit. *Nature* 2000;407:327–339. [PubMed: 11014182]
- Wool IG. Extraribosomal functions of ribosomal proteins. *Trends Biochem Sci* 1996;21:164–165. [PubMed: 8871397]
- Worbs M, Bourenkov GP, Bartunik HD, Huber R, Wahl MC. An extended RNA binding surface through arrayed S1 and KH domains in transcription factor NusA. *Mol Cell* 2001;7:1177–1189. [PubMed: 11430821]

- Worbs M, Huber R, Wahl MC. Crystal structure of ribosomal protein L4 shows RNA-binding sites for ribosome incorporation and feedback control of the S10 operon. *EMBO J* 2000;19:807–818. [PubMed: 10698923]
- Zellars M, Squires CL. Antiterminator-dependent modulation of transcription elongation rates by NusB and NusG. *Mol Microbiol* 1999;32:1296–1304. [PubMed: 10383769]
- Zengel JM, Jerauld A, Walker A, Wahl MC, Lindahl L. The extended loops of ribosomal proteins L4 and L22 are not required for ribosome assembly or L4-mediated autogenous control. *RNA* 2003;9:1188–1197. [PubMed: 13130133]

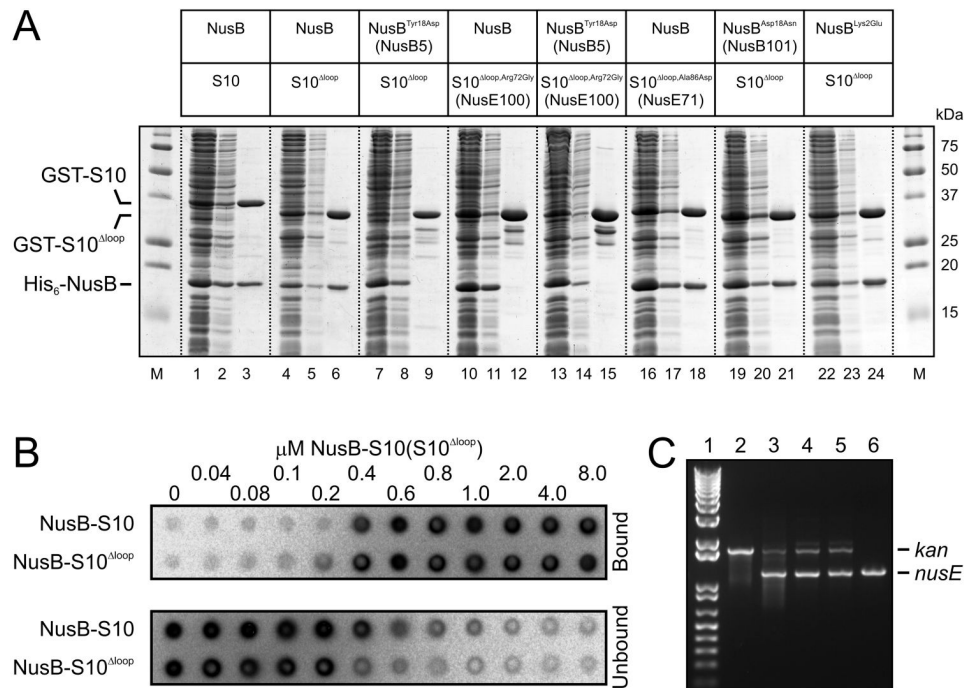


Figure 1. Analysis of the S10^{Δloop} Mutant

(A) Co-purification of GST-S10 or GST-S10^{Δloop} and mutants with His₆-NusB and mutants. Groups of three lanes show the soluble extract from co-overexpression experiments (first lane), the wash (second lane) and the elution (third lane) from glutathione beads. Co-expressed proteins are indicated above the group of lanes. M - molecular mass marker.

(B) Double filter-binding assays of a NusB-S10 complex to an *rrn* BoxA-containing 19mer RNA. Upper panel - nitrocellulose layer representing bound RNA. Lower panel - nylon filter representing unbound RNA. The upper lanes correspond to the full-length complex, the lower lanes to the NusB-S10^{Δloop} complex. Numbers indicate protein concentrations in μM.

(C) Gel analysis of *nusE* <> *kan* recombinants. Kanamycin resistant cells from a single colony were analyzed by PCR for configuration of the targeted chromosomal *nusE* region. Lane 1 - DNA marker (Invitrogen). Lanes 2 and 3 - PCR products from recombinant cells that contained pBAD*nusE*. Lanes 4 and 5 - PCR products from recombinant cells that contained pBAD*nusE*^{Δloop} initially selected either with (lanes 2 and 4) or without (lanes 3 and 5) 0.2 % arabinose. Lane 6 - PCR product control of wt *nusE* from the bacterial chromosome. Note that a haploid *nusE* <> *kan* knockout can be made only when pBAD*nusE* is induced by arabinose, *i.e.* when wt *nusE* is expressed from the plasmid (lane 2).

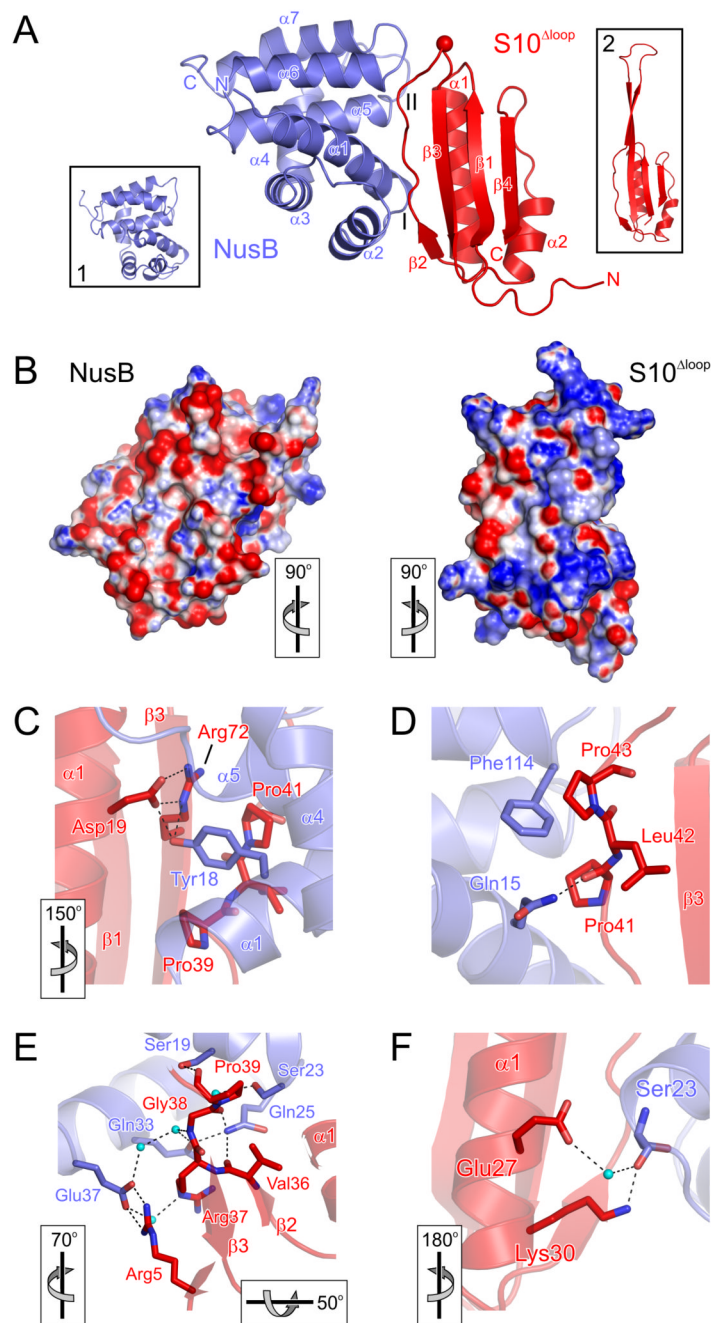


Figure 2. Structure of the NusB-S10^{Δloop} Complex

(A) Ribbon plot of the *E. coli* NusB-S10^{Δloop} complex. NusB - blue, S10^{Δloop} - red. Secondary structure elements and termini are labeled. The red sphere marks the site at which the ribosome-binding loop of S10 has been replaced by a single serine. I, II –interaction regions on the flank of the first three helix bundle (I) and on a tip of the second three helix bundle (II) of NusB. Inset 1 –NMR structure of *ecoNusB* (PDB ID 1EY1; (Altieri et al., 2000)) after global superpositioning on the NusB molecule of the present complex. Inset 2 - Structure of S10 from the *E. coli* 30S subunit (PDB ID 2AVY; (Schuwirth et al., 2005)) after global superpositioning on the S10^{Δloop} molecule of the present complex.

(B) Electrostatic surface potentials mapped on the surfaces of NusB (left) and S10^{Δloop} (right) showing a view on the interfaces of both molecules. Blue - positive charge, red - negative charge. Protomers were rotated 90° relative to panel (A) as indicated.

(C–F) Details of the NusB-S10^{Δloop} interaction. Interacting residues and secondary structure elements are labeled. Residues of interest are colored by atom type: carbon - as the respective molecules; oxygen - red; nitrogen - blue. Cyan spheres - water molecules. Dashed lines - hydrogen bonds or salt bridges. Views relative to Figure 2A are indicated.

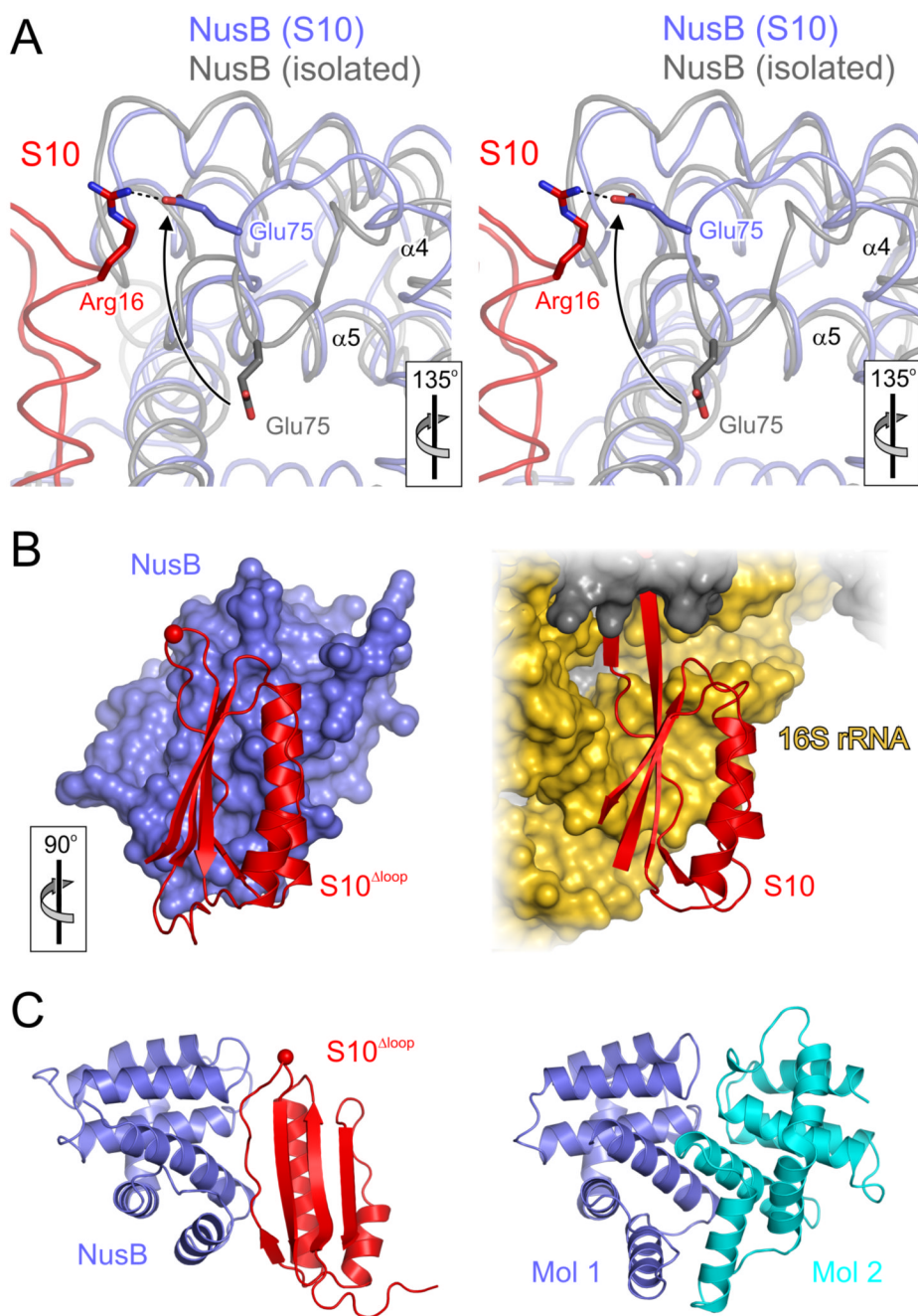


Figure 3. Aspects of the NusB-S10 Δ loop Interaction

(A) Stereo ribbon plot showing induced fit adjustment of the loop between helices $\alpha 4$ and $\alpha 5$ in NusB. An NMR structure of *E. coli* NusB (gray; PDB ID 1EY1; (Altieri et al., 2000)) was superimposed on the NusB subunit of the present NusB-S10 Δ loop complex (blue and red, respectively). The view relative to Figure 2A is indicated. Glu75 of NusB changes its position upon complex formation (arrow) in order to engage in a salt bridge with Arg16 of S10 Δ loop. Relevant residues are in sticks and colored by atom type as before.

(B) Comparison of S10 Δ loop (red) binding to NusB (blue) and S10 binding to the remainder of the 30S subunit (rRNA - gold; r-proteins - gray). The orientation relative to Figure 2A is indicated.

(C) Comparison of the present NusB-S10^{Δloop} complex (blue and red, left) with the *M. tuberculosis* NusB dimer (blue and cyan, right; PDB ID 1EYV; (Gopal et al., 2000)). The blue NusB molecules of both complexes are in the same orientation.

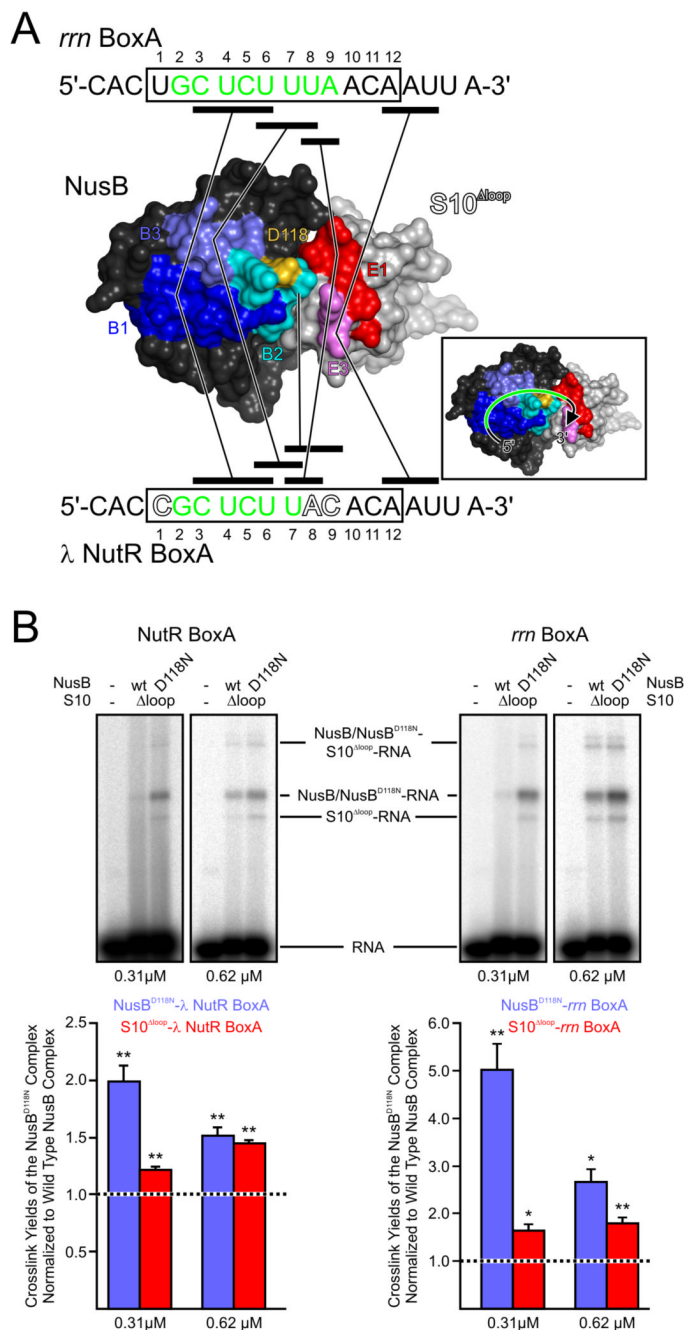


Figure 4. BoxA RNA Binding

(A) Mapping of crosslinked peptides on the surface of the NusB-S10^{Δloop} complex. The view is from the top of Figure 2A. NusB - dark gray, S10 - light gray. Crosslinked peptides of NusB (B1, B2, B3; see Table S3 for peptide sequences) are dark blue, cyan and steel blue, respectively. Crosslinked peptides of S10 (E1 and E3) are red and violet, respectively. Asp118 - gold. RNAs encompassing the *rrm* and λ BoxA elements and used for crosslinking are given above and below the structure, respectively. Boxed regions with residue numbers indicate the core BoxA elements. Residues in green of *rrm* BoxA RNA and λ BoxA RNA have previously been implicated in recruitment of NusB and S10 to antitermination complexes by mutational analysis (Mogridge et al., 1998). Outlined residues differ in λ BoxA compared to *rrm* BoxA.

Black bars designate crosslinked regions of the RNAs. They are connected by lines to the peptides, to which they have been crosslinked (Table S3). Inset 1 illustrates the deduced topology of the NusB-S10-BoxA RNA complexes.

(B) Top: Representative crosslinking of λ NutR BoxA RNA (left two panels) or *rrm* BoxA RNA (right two panels) to NusB-S10 Δ loop or NusB101-S10 Δ loop (NusB^{Asp118Asn}-S10 Δ loop). Two concentrations of protein complex (0.31 μ M and 0.62 μ M) were crosslinked, resolved on SDS gels and visualized by autoradiography. In each panel, RNA alone is in the left lane, NusB-S10 Δ loop complex in the central lane and NusB101-S10 Δ loop complex in the right lane. Bottom: Quantification of crosslink yields. Values are the crosslink yields of the protein components of the NusB101-S10 Δ loop samples, relative to the crosslink yields of the corresponding components of the NusB-S10 Δ loop samples. The crosslink yields of the components of the NusB-S10 Δ loop samples were set at 100 % (dashed lines). Values represent the mean of three independent experiments \pm the standard errors of the mean. Asterisks - p 0.032; double asterisks - p 0.020.

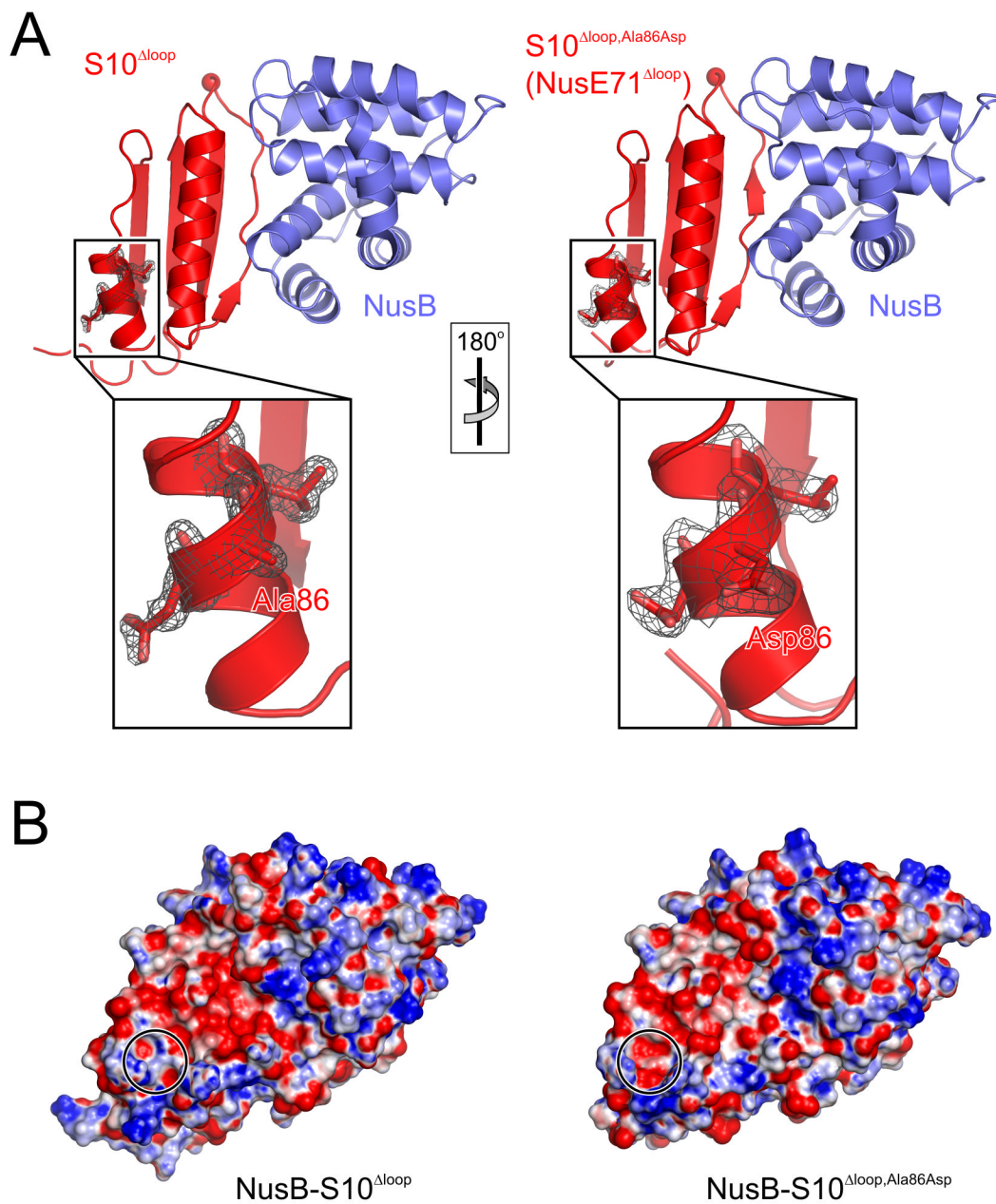


Figure 5. NusB-S10^{Δloop,Ala86Asp} Complex

(A) Comparison of the NusB-S10^{Δloop} complex (left) with the NusB-S10^{Δloop,Ala86Asp} complex (right). Gray meshes - final $2F_o - F_c$ electron densities covering residue 86 and neighboring residues of the S10^{Δloop} molecules, contoured at the 1σ level. Insets - closeup views of the residue 86 regions. The orientation relative to Figure 2A is indicated. (B) Comparison of the electrostatic surface potentials of the complexes. Blue - positive charge, red - negative charge. Left - NusB-S10^{Δloop} complex. Right - NusB-S10^{Δloop,Ala86Asp} complex. The positions of residue 86 are circled. The orientations are the same as in panel A.

Table 1*nusE*⁺ and *nusE*^{Δloop} Are Dominant to *nusE71*

Chromosomal <i>nusE</i>	pBAD Plasmid	Arabinose	λ EOP
+	-	-	1
71	-	-	<10 ⁻⁵
71	<i>nusB</i> ⁺	-	<10 ⁻³
71	<i>nusE</i> ⁺	-	1.0
71	<i>nusE</i> ^{Δloop}	-	1.0
71	<i>nusB</i> ⁺	+	<10 ⁻³
71	<i>nusE</i> ⁺	+	1.0
71	<i>nusE</i> ^{Δloop}	+	1.0

nusE71 is non-permissive for λ growth at 42 °C. Strains are W3102 derivatives that carry *nusE*⁺ or the *nusE71* mutation in the chromosome and the indicated plasmid. *λimm434* was titered on LB or LB plus ampicillin (50 μg/ml) at 42 °C and Efficiencies of Plating (EOP) were determined. Where indicated, 0.1 % arabinose was added to the plate.

Table 2

Crystallographic Data

Data Collection	NusB-S10 ^{Δloop}	NusB-S10 ^{Δloop,Ala86Asp}
Wavelength (Å)	0.9051	0.9763
Temperature (K)	100	100
Space Group	P2 ₁ 2 ₁ 2 ₁	I4 ₁ 22
Unit Cell Parameters (Å, °)	a = 40.7, b = 49.0, c = 122.8	a = b = 112.2, c = 266.2
Resolution (Å)	30.0–1.3 (1.4–1.3) ^a	50.0–2.6 (2.7–2.6)
Reflections		
Unique	56411 (11095)	26358 (2780)
Completeness (%)	100 (100)	100 (100)
Redundancy	15.3 (14.6)	7.1 (6.5)
I/σ(I)	17.5 (5.3)	19.8 (3.9)
R_{sym}(I) ^b	7.4 (64.8)	6.8 (46.2)
Refinement		
Resolution (Å)	20.0–1.3 (1.33–1.30)	30.0–2.6 (2.67–2.60)
Reflections		
Number	56394 (4109)	26337 (1921)
Completeness (%)	100 (100)	100 (100)
Test Set (%)	5.0	5.0
R_{work} ^c	17.3 (27.8)	21.8 (29.5)
R_{free} ^c	20.4 (29.7)	28.0 (35.8)
Refined Molecules/Atoms		
Protein	1 NusB, 1 S10 ^{Δloop} /1779	3 NusB, 3 S10 ^{Δloop,Ala86Asp} /5308
Water Oxygens	316	197
Solutes	3 CHES buffer molecules/39	-
Mean B-Factors (Å²)		
Wilson	24.6	54.3
Protein	21.5	48.7
Water	41.0	46.0
Ligand	38.2	-
Ramachandran Plot ^d		
Favored	99.1	96.8
Allowed	0.9	2.3
Outliers	0	0.9
RMSD ^e from Target Geometry		
Bond Lengths (Å)	0.013	0.006
Bond Angles (°)	1.51	1.09
RMSD B-Factors (Å²)		
Main Chain Bonds	0.86	0.28
Main Chain Angles	1.31	0.51
Side Chain Bonds	2.47	0.45
Side Chain Angles	3.58	0.80
PDB ID	3D3B	3D3C

^aData for the highest resolution shell in parentheses

^b $R_{\text{sym}}(I) = \frac{\sum_{hkl} \sum_i |I_i(hkl) - \langle I(hkl) \rangle|}{\sum_{hkl} \sum_i I_i(hkl)}$; for n independent reflections and i observations of a given reflection; $\langle I(hkl) \rangle$ - average intensity of the i observations

^c $R = \frac{\sum_{hkl} ||F_{\text{obs}}| - |F_{\text{calc}}||}{\sum_{hkl} |F_{\text{obs}}|}$; $R_{\text{work}} - hkl \notin T$; $R_{\text{free}} - hkl \in T$; T - test set

^dCalculated with MolProbity (<http://molprobity.biochem.duke.edu/>)

^eRMSD - root-mean-square deviation

Table 3Overproduction of S10 or S10^{Δloop} Restores λN and HK022 Nun Functions in a Δ*nusB* Strain

N-Antitermination			
Chromosomal <i>nusB</i>	pBAD Plasmid	Arabinose	λ EOP
+	-	-	1.0
Δ	-	-	<10 ⁻⁵
Δ	<i>nusE</i> ⁺	-	<10 ⁻²
Δ	<i>nusE</i> ^{Δloop}	-	<10 ⁻²
Δ	<i>nusE</i> ⁺	+	0.30
Δ	<i>nusE</i> ^{Δloop}	+	0.71
Nun-Termination			
HK022	pBAD	- Arabinose	+ Arabinose
-	<i>nusE</i>	2260	1453
-	<i>nusE</i> ^{Δloop}	2373	1856
+	<i>nusE</i>	951 (58)	213 (85)
+	<i>nusE</i> ^{Δloop}	1208 (49)	406 (78)

N antitermination: *nusE*⁺ and *nusE*^{Δloop} were carried by a pBAD plasmid and, where indicated, induced with 0.1 % arabinose. *λimm434*, which is insensitive to λ repressor, was plated at 37 °C on LB plates with or without (+/-) 50 μg/ml ampicillin to determine EOP. Strains are W3102 derivatives carrying the fusion *λcI857 - pR - cro* (ΔRBS) - *nutR - tR1 - cII::lacZ*. Nun termination: *nusB::Cam* cells additionally carried a HK022 prophage as indicated. Cells were grown at 37 °C until early log phase and then shifted to 42 °C for 2 hours without (“- Arabinose”) or with (“+ Arabinose”) 0.1 % arabinose. Numbers in parentheses indicate % termination.